Optimized Control Strategy Based on Dynamic Redundancy for the Modular Multilevel Converter

Gaoren Liu, Zheng Xu, *Member, IEEE*, Yinglin Xue, *Student Member, IEEE*, and Geng Tang

***Abstract*—Considering the synthetical effects of the ac system and the dc system, this paper proposes two novel indexes, the dynamic redundancy and the utilization ratio of the submodules. On this basis, the nearest level control is applied as the modulation method and an optimized control strategy based on the dynamic redundancy for the modular multilevel converter (MMC) is proposed. One of the main innovations is that the reference value of the capacitor voltage is derived according to the maximum output voltage of each converter arm and the safety margin which can be adjusted artificially. Unlike previous strategies, the redundancy can be adjusted dynamically, and the utilization ratio of the submodules can be effectively improved. In addition, the capacitor voltage and the inner stress are reduced, and the fault ride-through capability of the system can be enhanced. In particular, the strategy under abnormal operating conditions is also detailed in this paper. A model of two-terminal MMC-high-voltage direct current system is built in PSCAD/EMTDC, and the simulation result proves the validity and the feasibility of the proposed strategy.**

***Index Terms*—AC redundancy, dc redundancy, dynamic redundancy, modular multilevel converter (MMC), redundancy protection, utilization ratio of sub-modules.**

NOMENCLATURE

L_0	Arm inductance.
$U_{\rm dc}$	DC-bus voltage.
u_j $(j = a, b, c)$	AC-side phase to ground voltage.
u_o	Potential to ground of point "o."
u_N	Potential to ground of point "N."
$U_{c,k}$ $(k = p, n)$	SM capacitor voltage in the corresponding arm.
$U_{{\rm sm},i}$	Output voltage for the ith SM.
$U_{{\rm arm},k}$ $(k = p, n)$	Output voltage of the corresponding arm.
$\hat{U}_j$	Amplitude of u_j.
$\hat{U}_{\rm arm}$	Amplitude of $U_{\rm arm}$.
$U_{\rm crated}$	Rated SM capacitor voltage.
$U_{\rm cref}$	Reference value of the capacitor voltage.
$U_{\rm armref}$	Reference value of the arm voltage.
$N_{\rm dc}$	Number of dc-redundant SMs.
$R_{\rm dc}$	DC redundancy.
$N_{\rm ac}$	Number of ac-redundant SMs.
$R_{\rm ac}$	AC redundancy.
$R_{\rm dynamic}$	Dynamic redundancy.
γ	Utilization ratio of SMs.
$N_{\rm rated}$	Rated Number of SMs per arm.
$N_{\rm total}$	Total number of arm SMs.
$N_{\rm basic}$	Maximum number of inserted SMs when the system operates under traditional strategy.
$N_{\rm max}$	Maximum number of on-state SMs when the system operates under optimized strategy.
$U'_{\rm cref}$	Reference value of the capacitor voltage under the optimized strategy.
$U_{\rm dc\_ref}$	Reference value of $U_{\rm dc}$.
$u_{j\_{\rm ref}}$	Reference value of u_j.
$u_{\rm diff}$	Actual value of the circulating current suppression component.
$u_{\rm diff\_ref}$	Reference value of the circulating current suppression component.
$N_{\rm tolerate}$	Capability of fault-tolerance.

Manuscript received July 1, 2013; revised September 21, 2013, October 31, 2013, December 10, 2013, and January 14, 2014; accepted February 3, 2014. Date of publication February 19, 2014; date of current version August 26, 2014. This work was supported by the National High Technology Research and Development Program of China under Project 2012AA050205. Recommended for publication by Associate Editor S. Bernet.

The authors are with the Department of Electrical Engineering, Zhejiang University, Hangzhou 310027, China (e-mail: liugaoren@zju.edu.cn; xuzheng007@zju.edu.cn; yinglinxue@gmail.com; tanggeng7@zju.edu.cn).

Digital Object Identifier 10.1109/TPEL.2014.2305663

I. INTRODUCTION

WITH the rapid growth of power demand and the development of power electronic technology, the high-voltage direct current (HVDC) system based on the modular multilevel converter (MMC) topology has attracted widespread attention. The MMC was first introduced in 2001 [1]. Due to the modular construction, series connection of power electronic devices is avoided, and the requirement for dynamic voltage equalization is lowered [2]–[4]. In addition, the active and reactive power can be controlled separately, and the operating cost is quite low [5]–[8]. All these characters make an MMC a competitive topology for applications in HVDC and flexible ac transmission systems [9].

The basic structure of a three-phase MMC is shown in Fig. 1. Because of the high dc-bus voltage, in practical engineering, each converter arm consists of a large number of submodules (SMs) (e.g., "Trans Bay Cable" Project, the first commercial MMC-HVDC project in the world, is reported to have about 216 SMs per arm [10]), which greatly increases the probability of SM failures. SM fault is one of the main risks in an MMC. When an SM malfunctions, the normal operation of the converter will be affected, and the system may endure a transient impact. Therefore, in order to enhance the robustness of the system, the fault protection method must be added to the system. In an actual operation, a number of redundant SMs are usually integrated into the arm to make the system operate redundantly [11].

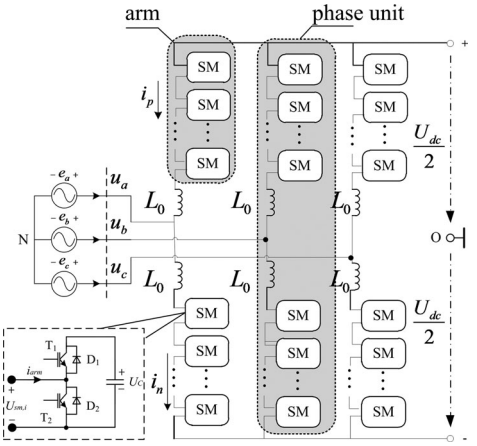

Fig. 1. Circuit configuration of the MMC.

So far, most studies focused on the modulation and control of the MMC without taking redundant SMs into consideration [12]–[20]. Konstantinou *et al*. [11] discuss the operation of an MMC when redundant SMs are utilized and analyzes the impact on the switching frequency. A control strategy of an MMC considering redundant SMs and SM faults is proposed in [21]. Although the strategy is feasible for noninterruptible energy transfer, the SMs will not be fully utilized in the method.

In the existing strategies, although the reference value of the capacitor voltage $U_{\rm cref}$ is not mandatory coupled to the dc-bus voltage, it is often set or adjusted within a narrow range, especially in the real MMC-HVDC systems. In addition, in order to reserve adequate margin for the fluctuation of the ac voltage, the control strategy is always designed under the assumption that the ac voltage reaches its maximum value, which means that $U_{\rm cref}$ is mainly affected by the dc-bus voltage and the rated number of SMs (without considering the redundant SMs). This makes the capacitor voltage of SMs relatively high, which increases the voltage stress in insulated gate bipolar transistors (IGBTs) and capacitors, and reduces the lifespan of SMs. In addition, as the modulation index decreases, the requisite number of SMs per arm (i.e., the maximum number of inserted SMs) will decrease proportionally, which means that the actual redundancy is affected by both ac and dc sides. If the modulation index is fairly low, the actual redundancy will remain at a quite high level, and the maximum utilization ratio of SMs will be greatly reduced.

In this paper, an optimized control strategy based on dynamic redundancy for the MMC with redundant SMs is proposed. One of the main innovations is that the reference value of the capacitor voltage is self-adaptive according to a particular dynamic redundancy which can be adjusted artificially. In this method, the utilization ratio of SMs can be improved effectively, and the capacitor voltage is reduced. The rest of this paper is organized as follows. Section II introduces the basic structure and the operation principle of the MMC. Considering the synthetical effects of ac and dc systems, two indexes—the dynamic redundancy and the utilization ratio of SMs—are proposed in Section III. In addition, the optimized modulation is also introduced in this part. Section IV discusses the self-adaptive characteristics of the capacitor voltage and the way to adjust the redundancy dynamically under normal or abnormal conditions. To verify the validity and the feasibility of the proposed method, the simulation studies in PSCAD/EMTDC are presented in Section V. The conclusions are given in Section VI.

II. Basic Structure and the Operation Principle of the MMC

Fig. 1 shows the basic structure of a three-phase MMC. u_o is the potential to ground of point "o," which is considered as the dc-side neutral point and unavailable in a realistic MMC-HVDC system [6], [17]. Point "N" is the neutral point of the grid in the valve side, and its potential to ground is u_N. The converter consists of six arms, each having a series connection of $N_{\rm total}$ nominally identical half-bridge SMs and one inductor L_0, and the upper and lower arms in the same leg comprise a phase unit. Each SM is composed of two IGBT switches, two antiparallel diodes, and a capacitor. $U_{\rm dc}$ is the total dc-bus voltage and u_j $(j = a, b, c)$ is the ac-side phase to ground voltage of phase j in the valve side.

The voltage balancing strategy is usually applied to reduce the voltage ripple in an individual SM and balance the capacitor voltages among all the SMs in the same arm. At a reasonable switching frequency, such as 200–300 Hz, the variations among the capacitor voltages in the same arm can be limited to within 3% [22]. Thus, the capacitor voltage of each SM in a given arm can be considered to be the same. For phase j, it can be defined as $U_{c,p}$ or $U_{c,n}$ respectively, where the subscripts p and n denote the upper and lower arms. For the ith SM, the output voltage $U_{{\rm sm},i}$ can be expressed as

$$U_{{\rm sm},i} = \begin{cases} S_{i,p} \times U_{c,p} & \text{(in the upper arm)} \\ S_{i,n} \times U_{c,n} & \text{(in the lower arm)} \end{cases} \tag{1}$$

where $S_{i,p}$ and $S_{i,n}$ denote the switching function of the ith SM in the corresponding arm. When $S_{i,p} = 1$ (or $S_{i,n} = 1$), T1 is switched ON and T2 is switched OFF, the SM is working in the on-state; when $S_{i,p} = 0$ (or $S_{i,n} = 0$), T1 is switched OFF and T2 is switched ON, the SM is working in the off-state.

According to the Kirchhoff's voltage law, the arm voltage $U_{{\rm arm},p}$ and $U_{{\rm arm},n}$ for phase j can be expressed as [17]

$$\begin{aligned} U_{{\rm arm},p} &= \frac{1}{2}U_{\rm dc} + u_o - u_j \\ &= \sum_{i=1}^{N_{\rm total}} (S_{i,p} \times U_{c,p}) + L_0 \frac{{\rm d}i_p}{{\rm d}t} \end{aligned} \tag{2a}$$

$$\begin{aligned} U_{{\rm arm},n} &= \frac{1}{2}U_{\rm dc} - u_o + u_j \\ &= \sum_{i=1}^{N_{\rm total}} (S_{i,n} \times U_{c,n}) + L_0 \frac{{\rm d}i_n}{{\rm d}t} \end{aligned} \tag{2b}$$

where i_p and i_n are the arm currents, respectively. Assuming that u_j consists of a sinusoidal component added with u_N, which can be expressed as

$$u_j = \hat{U}_j \sin(\omega t + \theta) + u_N. \tag{3}$$

Since the voltage drop over L_0 is quite small compared to the dc-bus voltage, we can approximately obtain

$$\sum_{i=1}^{N_{\text{total}}} (S_{i,p} \times U_{c,p}) = \frac{1}{2}U_{\text{dc}} + u_o - \hat{U}_j \sin(\omega t + \theta) - u_N \quad (4a)$$

$$\sum_{i=1}^{N_{\text{total}}} (S_{i,n} \times U_{c,n}) = \frac{1}{2}U_{\text{dc}} - u_o + \hat{U}_j \sin(\omega t + \theta) + u_N. \quad (4b)$$

According to the basic principle of the MMC, the upper and lower arms should generate complementary-symmetry voltages to provide an appropriate ac-side voltage in normal operations [3]. In the commonly used method, $U_{\text{arm},p}$ and $U_{\text{arm},n}$, which can be considered as the sum of $U_{\text{sm},i}$ in the corresponding arm if the voltage drop over L_0 is still ignored, can be expressed as $(U_{\text{dc}}/2 - \hat{U}_{\text{arm}} \sin(\omega t + \theta))$ and $(U_{\text{dc}}/2 + \hat{U}_{\text{arm}} \sin(\omega t + \theta))$, respectively, [23], where $\hat{U}_{\text{arm}}$ is the amplitude of the arm voltage. Substituting the analyses above into (4a) and (4b) and comparing both sides of the equations, it can be approximately obtained that $\hat{U}_{\text{arm}}$ equals $\hat{U}_j$ and u_N equals u_o. Hence, (4a) and (4b) can be rewritten as

$$\sum_{i=1}^{N_{\text{total}}} (S_{i,p} \times U_{c,p}) = \frac{1}{2}U_{\text{dc}} - \hat{U}_j \sin(\omega t + \theta) \quad (5a)$$

$$\sum_{i=1}^{N_{\text{total}}} (S_{i,n} \times U_{c,n}) = \frac{1}{2}U_{\text{dc}} + \hat{U}_j \sin(\omega t + \theta). \quad (5b)$$

The arm voltages are basically limited by the number of configured SMs, to be specific, the arm voltage will range from 0 to $N_{\text{total}} \times U_{c,k}$ ($k = p, n$). Thus, the capacitor voltage has to fulfill the requirements in (5a) and (5b)

$$\frac{1}{2}U_{\text{dc}} - \hat{U}_j \le \sum_{i=1}^{N_{\text{total}}} (S_{i,p} \times U_{c,p}) \le \frac{1}{2}U_{\text{dc}} + \hat{U}_j \le N_{\text{total}} \times U_{c,p} \quad (6a)$$

$$\frac{1}{2}U_{\text{dc}} - \hat{U}_j \le \sum_{i=1}^{N_{\text{total}}} (S_{i,n} \times U_{c,n}) \le \frac{1}{2}U_{\text{dc}} + \hat{U}_j \le N_{\text{total}} \times U_{c,n}. \quad (6b)$$

The amplitude modulation index m, for phase j, can be expressed as

$$m = \frac{\hat{U}_j}{U_{\text{dc}}/2}. \quad (7)$$

Substituting (7) into (6a) and (6b), the equations can be rewritten as

$$\frac{1}{2}U_{\text{dc}}(1-m) \le \sum_{i=1}^{N_{\text{total}}} (S_{i,p} \times U_{c,p}) \le \frac{1}{2}U_{\text{dc}}(1+m) \le N_{\text{total}} \times U_{c,p} \quad (8a)$$

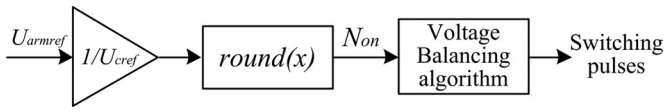

Fig. 2. Control diagram of the NLC method.

$$\frac{1}{2}U_{\text{dc}}(1-m) \le \sum_{i=1}^{N_{\text{total}}} (S_{i,n} \times U_{c,n}) \le \frac{1}{2}U_{\text{dc}}(1+m) \le N_{\text{total}} \times U_{c,n}. \quad (8b)$$

Hence, we can obtain the basic requirement of the capacitor voltage

$$U_{c,k} \ge \frac{1}{2}\frac{U_{\text{dc}}(1+m)}{N_{\text{total}}} \quad (k = p, n). \quad (9)$$

In industrial applications, the nearest level control (NLC) is often chosen for the modulation process [24]. The control diagram of the NLC method is depicted in Fig. 2, where U_{cref} is the reference value of the capacitor voltage, or can be approximately considered as the mean value, and U_{armref} is the reference value of the arm voltage of the corresponding arm. In this method, the number of SMs which should be inserted per arm can be expressed as

$$\sum_{i=1}^{N_{\text{total}}} S_{i,p} \le \frac{1}{2}\frac{U_{\text{dc}}(1+m)}{U_{\text{cref}}} \quad (10a)$$

$$\sum_{i=1}^{N_{\text{total}}} S_{i,n} \le \frac{1}{2}\frac{U_{\text{dc}}(1+m)}{U_{\text{cref}}}. \quad (10b)$$

Under an appropriate voltage balancing strategy, the fluctuation of the capacitor voltage in an individual SM can be limited to around 5% [22]. In addition, the fundamental fluctuation, which accounts for the largest proportion, is reversed in the upper and lower arms [25]. Hence, when adding (5a) and (5b) together, the voltage fluctuations in the two arms will be majorly offset and $U_{c,k}$ can be approximately replaced by U_{cref}. We can obtain

$$\sum_{i=1}^{N_{\text{total}}} S_{i,p} + \sum_{i=1}^{N_{\text{total}}} S_{i,n} \approx \frac{U_{\text{dc}}}{U_{\text{cref}}}. \quad (11)$$

Equation (10a), (10b), and (11) are the basic principles of SM configuration.

III. Modulation Scheme Based on Dynamic Redundancy

A. Influence on SM Operations from AC and DC Systems

Normally, the rated number of SMs per arm (without regard to the redundant SMs) is determined by the dc-bus voltage and the rated capacitor voltage U_{crated} of the SMs

$$N_{\text{rated}} = \text{ceil}\left(\frac{U_{\text{dc}}}{U_{\text{crated}}}\right) \quad (12)$$

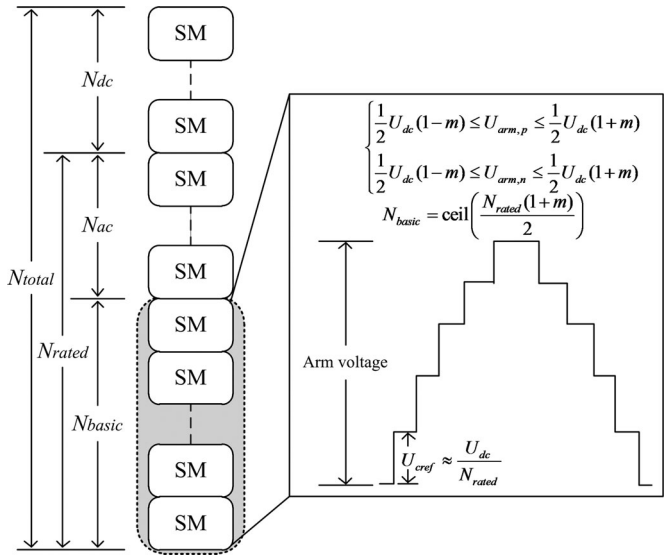

Fig. 3. Operation of the MMC in a traditional way.

where ceil(x) represents the smallest integer not less than the real number x. In traditional methods, the reference value of the capacitor voltage $U_{\rm cref}$ is usually equal to $U_{\rm crated}$.

When $m = 1$, according to (10a) and (10b), the number of the SMs which should be working in the on-state ranges from 0 to $N_{\rm rated}$, and the arm voltage ranges from 0 to $U_{\rm dc}$. This means that the number of SMs per arm must be greater than or equal to $N_{\rm rated}$. On this basis, the additionally inserted SMs are called redundant SMs in the traditional sense. Since $N_{\rm rated}$ SMs have already met the constraint of the dc-bus voltage, in this condition, the redundant SMs can be called the dc-redundant SMs, whose number is $N_{\rm dc}$. The dc redundancy can be defined as

$$R_{\rm dc} = \frac{N_{\rm dc}}{N_{\rm rated}}. \tag{13}$$

When $m < 1$, if the dc-redundant SMs are ignored temporarily, $N_{\rm basic}$ (the maximum requisite number of SMs when the system operates normally) will change to ceil $\left(\frac{1}{2}N_{\rm rated}(1+m)\right)$. This means that the arm SMs will not be fully utilized and there will be at least floor $\left(\frac{1}{2}N_{\rm rated}(1-m)\right)$ SMs working in the off-state at any given moment, where floor (x) represents the largest integer not greater than the real number x. In this condition, the generation of the redundancy is caused by the ac side, to be specific, the amplitude of the ac phase voltage is less than the dc-bus voltage. Hence, the redundant SMs here can be called the ac-redundant SMs, whose number is $N_{\rm ac}$. The ac redundancy can be defined as

$$R_{\rm ac} = \frac{N_{\rm ac}}{N_{\rm rated}} = \frac{1}{2}(1-m). \tag{14}$$

As shown in Fig. 3, the relationship of $N_{\rm total}$ (the total number of arm SMs), $N_{\rm dc}, N_{\rm ac}, N_{\rm rated}$, and $N_{\rm basic}$ can be expressed as

$$N_{\rm basic} = \text{ceil}\left(\frac{1}{2}N_{\rm rated}(1+m)\right) \tag{15}$$

$$N_{\rm basic} + N_{\rm ac} = N_{\rm rated} \tag{16}$$

$$N_{\rm rated} + N_{\rm dc} = N_{\rm total}. \tag{17}$$

It can be seen that, $N_{\rm total}, N_{\rm dc}$, and $N_{\rm rated}$ are all fixed and determined by the initial configuration, while $N_{\rm basic}$ and $N_{\rm ac}$ are influenced by the ac-side voltage. In the case of $m < 1$, each arm only needs $N_{\rm basic}$ SMs in total, all the rest can be regarded as redundant SMs, whose number is $N_{\rm ac} + N_{\rm dc}$. In practical applications, the modulation index is often set as 0.85, if $R_{\rm dc}$ is set as 10%, then the total redundancy (the sum of $N_{\rm ac}$ and $N_{\rm dc}$) will reach 17.5%. The utilization ratio of SMs can be defined as

$$\gamma = \frac{\text{the maximum number of the needed SMs per arm}}{N_{\rm total}}. \tag{18}$$

The utilization ratio of SMs in this condition is only 84.1%, which indicates the control strategy of SMs can be further optimized.

B. Optimized Modulation

The modulation and operation strategy of SMs has been studied in many aspects. In traditional methods, regardless of whether the redundant SMs are involved in switching operations, at least $N_{\rm rated}$ SMs must be guaranteed in each phase to withstand the dc-bus voltage, and the value of $N_{\rm rated}$ is determined by (12).

In addition, in order to reserve adequate margin for the fluctuation of the ac voltage, the control strategy is always designed under the assumption that m equals 1, which means that only the voltage and safety margin of the dc side are taken into consideration. This kind of strategy affects the utilization of SMs and leads to a series of drawbacks: 1) under a given operating condition, the ac-side voltage is approximately constant and lower than 1, which makes the total redundancy maintain at an unnecessarily high level, and lowers the utilization ratio of SMs; 2) the capacitor voltage in an individual SM is usually fluctuating around $U_{\rm dc}/N_{\rm rated}$ or adjusted within a narrow range, the relatively high voltage increases the voltage stress in the capacitor and the IGBTs, and the lifespan of SMs is reduced; 3) the redundant SMs do not contribute to the number of voltage levels, the voltage level and the total harmonic distortions could be optimized. Especially, under some special operating conditions, such as the load is relatively heavy or the station absorbs too much reactive power, m will be fairly low and the shortcomings will be aggravated.

To overcome the drawbacks noted previously, an optimized strategy which considers effects of the ac system is proposed here. As a novel index, the dynamic redundancy $R_{\rm dynamic}$ can be defined as

$$R_{\rm dynamic} = \frac{N_{\rm total} - N_{\rm max}}{N_{\rm rated}} \tag{19}$$

where $N_{\rm max}$ denotes the maximum number of on-state SMs when the system operates under the optimized strategy. The dynamic redundancy is a variable value which can be set artificially, and it denotes the ratio between the number of SMs which need not to be involved in voltage support and $N_{\rm rated}$. Generally, $R_{\rm dynamic}$ is inversely proportional to γ, and it reflects the synthetical redundancy affected by both ac and dc sides.

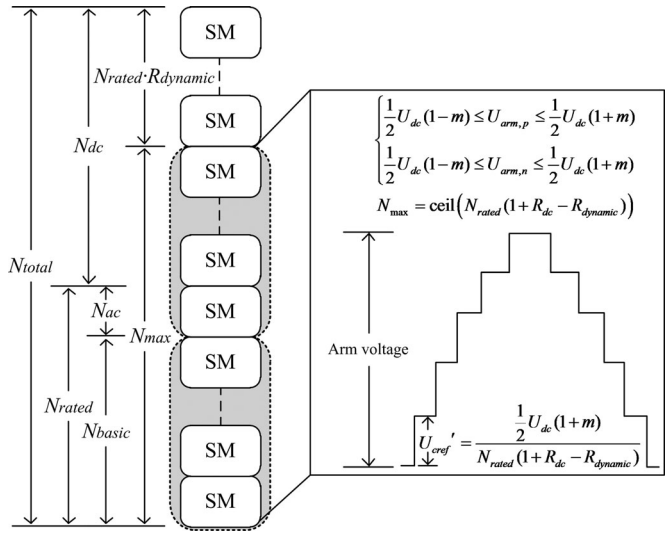

Fig. 4. Operation of the MMC under optimized strategy.

$N_{\max}$ and N_{basic} are both variable quantities and they denote the maximum requisite number of SMs under different strategies, respectively. But unlike $N_{\text{basic}}, N_{\max}$ only depends on R_{dynamic} and it is larger than N_{rated} in most conditions. $N_{\max}$ can be expressed by R_{dynamic} as

$$N_{\max} = \text{ceil}\left(N_{\text{rated}}(1 + R_{\text{dc}} - R_{\text{dynamic}})\right). \tag{20}$$

According to the analysis in Section II, it is not the dc-bus voltage that constrains the requisite number of on-state SMs, but the sum of $\frac{1}{2}U_{\text{dc}}$ and $\hat{U}_j$, and the system can operate normally as long as the maximum output voltage of the arm SMs (can be considered approximately as the arm voltage) meets this requirement. Hence, the utilization ratio of SMs can be improved through lowering the reference value of the capacitor voltage. As shown in Fig. 4, under a certain dynamic redundancy, the reference value of the capacitor voltage changes to

$$\begin{aligned} U'_{\text{cref}} &= \frac{\frac{1}{2}U_{\text{dc}}(1+m)}{N_{\max}} \approx \frac{U_{\text{dc}}}{N_{\text{rated}}} \frac{1+m}{2(1+R_{\text{dc}} - R_{\text{dynamic}})} \\ &= \frac{U_{\text{cref}}(1+m)}{2(1+R_{\text{dc}} - R_{\text{dynamic}})}. \end{aligned} \tag{21}$$

Substituting (21) into (10a) and (10b), the number of on-state SMs in the upper or lower arm under NLC method can be expressed as

$$\sum_{i=1}^{N_{\text{total}}} S_{i,p} \le N_{\text{rated}}(1 + R_{\text{dc}} - R_{\text{dynamic}}) \tag{22a}$$

$$\sum_{i=1}^{N_{\text{total}}} S_{i,n} \le N_{\text{rated}}(1 + R_{\text{dc}} - R_{\text{dynamic}}). \tag{22b}$$

As shown in Fig. 4, in the optimized modulation, the redundant SMs are not only involved in the switching operations, but also inserted to support the arm voltage. The increase of $N_{\max}$ and the decrease of U_{cref} can be expressed as

$$\Delta N_{\max} = \text{ceil}\left(N_{\text{rated}}\left(\frac{1}{2} + R_{\text{dc}} - R_{\text{dynamic}} - \frac{m}{2}\right)\right) \tag{23}$$

$$\Delta U_{\text{cref}} = U_{\text{cref}} \frac{1 + 2R_{\text{dc}} - 2R_{\text{dynamic}} - m}{2(1 + R_{\text{dc}} - R_{\text{dynamic}})}. \tag{24}$$

The number of on-state SMs in each phase changes to

$$\sum_{i=1}^{N_{\text{total}}} S_{i,p} + \sum_{i=1}^{N_{\text{total}}} S_{i,n} = \text{ceil}\left(\frac{2N_{\text{rated}}}{1+m}(1 + R_{\text{dc}} - R_{\text{dynamic}})\right). \tag{25}$$

The specific figure is related to R_{dynamic} and m. From the analyses shown previously, it can be seen that R_{dynamic} and γ are the two major indexes of the optimized strategy, and they can be regulated through the adjustment of U_{cref}.

IV. Control Strategy and Fault Protection

A. Dynamic Adjusting of Redundancy

From what has been discussed previously, it can be seen that the main improvement of the optimized modulation is the way how to calculate the U_{cref}. According to (21), a particular capacitor voltage corresponds to a particular dynamic redundancy. In fact, in order to enhance the flexibility of the system, the dynamic redundancy can be adjusted dynamically based on the self-adaptive characteristics of the capacitor voltage.

For instance, in a two-terminal MMC-HVDC system, the main function of the master station is to keep the dc-bus voltage at around U_{dc}. At a given moment, if the reference value of the capacitor voltage changes, the number of the SMs which should be inserted will be changed correspondingly. Since the capacitor voltage could not change too much in an instant, the arm voltage will no longer be equal to U_{dc}. With the help of the dc-voltage control strategy, the arm current will be adjusted to charge or discharge the capacitor so that the difference will be reduced and the capacitor voltage will reach the reference value eventually. Under this mechanism, the reference value of the capacitor voltage can be followed automatically, and this kind of characteristic can be called the self-adaptive characteristic.

Fig. 5 shows the block diagram of the NLC method based on dynamic redundancy. The reference value of the arm voltage is calculated according to (2a) and (2b). $U_{\text{dc\_ref}}$ is the reference value of U_{dc}, u_{j_ref} is the reference value of u_j, and u_{o_ref} is the reference value of u_o. Under actual operating conditions, the three parallel connected phase units may have different voltages, which lead to circulating currents among the three phase units [26]. The circulating currents will cause a series of drawbacks, thus the circulating current suppressing controller (CCSC) is added here [22]. In the CCSC, u_{diff} and $u_{\text{diff\_ref}}$ are the actual and reference value of the circulating current suppression component, respectively.

Under the optimized strategy, U_{cref} can be adjusted corresponding to a particular m and R_{dynamic}. To be specific, U_{cref} positively correlates with m and R_{dynamic}. Because of the

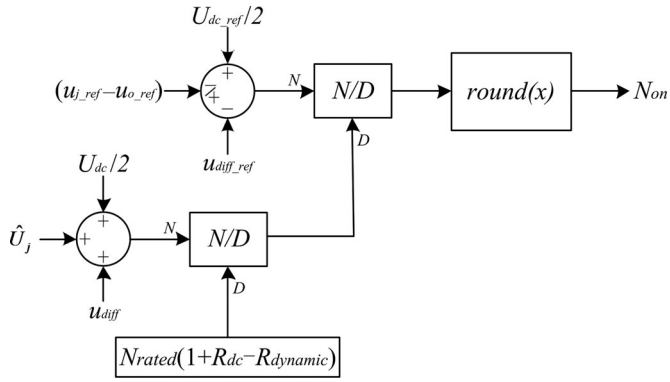

Fig. 5. NLC method based on dynamic redundancy.

self-adaptive characteristic, the dynamic adjusting of redundancy can be achieved.

Under a certain operating condition, a reasonable R_{dynamic} can be set according to the operating status: if the converter is working in the test state or has just suffered from a fault, the safety margin should be expanded to ensure the normal operation, therefore, R_{dynamic} should be increased appropriately; if the converter is working in the low-load condition or just completed the equipment maintenance, in order to improve the utilization ratio of SMs, R_{dynamic} should be reduced. Furthermore, when the operating condition of the ac system changes, such as the under-voltage operation, R_{dynamic} should be determined according to the actual change of m to ensure the stability of the system.

B. Fault Protection

In traditional strategies, when an SM fails, the faulted SM needs to be shorted out by the bypass switch and a normal SM should be inserted instead. The reference value of the capacitor voltage holds its original value, and the redundancy decreases accordingly. In engineering applications, if all dc-redundant SMs are inserted, the converter station must be taken out of operation. The number of the maximum tolerable faults is N_{dc}.

Unlike previous methods, all arm SMs are involved in the switching operation under the optimized strategy, and the reference value of the capacitor voltage is decided not only by the rated number of SMs but also the redundant SMs. At this point, there is no distinction between redundant SMs and the normal SMs in the strict sense. When an SM fails, the fire signal of the IGBT must be blocked immediately, and then the faulted SM must be bypassed to prevent the transient impact on the system. In this case, to keep the stability of the dc-bus voltage, U_{cref} should be recalculated as shown in Fig. 5 under a certain R_{dynamic}.

If the number of faulty SMs is relatively low, there is no need to reduce the R_{dynamic}, so the actual value of the capacitor voltage will rise with the increase of U_{cref}. According to (21), the voltage will return to the rated value, $U_{\mathrm{dc}}/N_{\mathrm{rated}}$, if the number of faulty SMs reaches ΔN

$$\Delta N = \mathrm{ceil}\left(\frac{N_{\mathrm{rated}}}{2}\left(\frac{1-m+2R_{\mathrm{dc}}-2R_{\mathrm{dynamic}}}{1+R_{\mathrm{dc}}-R_{\mathrm{dynamic}}}\right)\right). \tag{26}$$

If in this state a further SM fails, the adjustment of U_{cref} needs to be blocked to ensure that the capacitor voltage would not exceed the rated value, and R_{dynamic} should be reduced. When R_{dynamic} has reached zero, the system must be taken out of operation. The number of the maximum tolerable faults under this strategy is $N_{\mathrm{ac}}+N_{\mathrm{dc}}$.

Compared with the old strategy, the capability of fault-tolerance is increased by $\Delta N_{\mathrm{tolerate}}$

$$\Delta N_{\mathrm{tolerate}} = N_{\mathrm{ac}} = \mathrm{floor}\left(\frac{N_{\mathrm{rated}}(1-m)}{2}\right). \tag{27}$$

If the capacitor voltage is allowed to float upward in certain limit, $\Delta N_{\mathrm{tolerate}}$ will be greater than N_{ac}. As can be seen, the optimized method can effectively improve the fail-safe functionality of the system.

C. Control Under Special Operating Conditions

Since an MMC is able to support the voltage of the ac side by injection of proper reactive currents, in the case of the steady-state operation, the modulation index m will remain at a constant value. However, under certain conditions, the amplitude of the ac phase voltage will change dramatically in a short time. This will affect the calculation of U_{cref}, and become a threat to the stability of the system.

For transient fluctuations, such as switching overvoltage and power frequency overvoltage, the fluctuations occur and vanish in a short time, and the rate of voltage change is relatively high. If using the real-time value of the ac phase voltage to calculate U_{cref}, the number of SMs which need to be inserted will generate a step change. Since the self-adaptive process of the capacitor voltage will take some time, there will be a large deviation between the actual arm voltage and the desired output voltage, which makes the performances of the system fluctuate significantly.

For a permanent ground fault, the converter must be blocked and there is no need to adjust U_{cref}. If the fault is a temporary failure, such as a temporary single line-to-ground fault, the system should have the fault ride-through capability. In this case, the change of capacitor voltage should be minimized, and wait for the recovering.

Therefore, in order to deal with the special operating conditions, some additional improvements should be added as shown in Fig. 6. In the diagram, a rate limiter is added in the tracking block of the ac phase voltage to minimize the effects of the instantaneous voltage fluctuation; a hard limiter is added in the output block of U_{cref} to ensure that the capacitor voltage fluctuates within a reasonable range. Besides, a fault diagnosis block is added. When a fault is detected, the adjustment of the capacitor voltage will be blocked and U_{cref} remains unchanged until the fault is cleared.

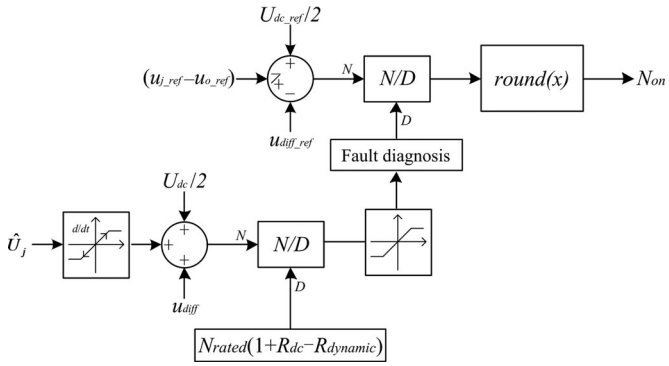

Fig. 6. Improved NLC method based on dynamic redundancy.

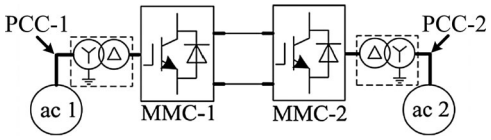

Fig. 7. Schematic diagram of the testing system.

TABLE I
MAIN CIRCUIT PARAMETERS OF THE TESTING SYSTEM

Items	Values	Comments
dc-bus voltage $U_{dc}/2$	±200kV	1.0 pu
Active power P	400MW	1.0 pu
ac system voltage $\hat{U}_{sj}$	93.5kV	
ac system inductance L_s	10mH	
Transformer ratio	110kV/200kV	Y_0/Δ
Transformer leakage inductance L_T	19.2mH	0.1 pu
Modulation index m	0.85	
Rated number of SMs per arm N_{rated}	200	
Number of dc-redundant SMs N_{dc}	20	
SM capacitance	24500μF	
Rated capacitor voltage U_{crated}	2kV	
Arm inductance L_0	29.3mH	0.13 pu

V. CASE STUDY

A. Study System

To verify the validity and the feasibility of the proposed method, a two-terminal MMC-HVDC model is established with the time-domain simulation tool PSCAD/EMTDC. A "nested fast and simultaneous solution" algorithm [27] is used to reduce the computational time without sacrificing any accuracy. The method does not make use of approximate interfaced models, and it maintains the individual identity of every SMs during the simulation.

The system structure is shown in Fig. 7, the main circuit parameters are listed in Table I. MMC-1 controls the dc-side voltage and reactive power and MMC-2 regulates the active and reactive power. Both stations operate at unity power factor and 400-MW active power transmits from MMC-1 to MMC-2. The NLC method is chosen for the modulation process, and in order to reduce the average device switching frequency, a reduced switching-frequency voltage balancing algorithm [22] is applied.

TABLE II
COMPARISON OF SOME OPERATING INDEXES

	Traditional strategy	Optimized strategy	Rate of change
Capacitor voltage /kV	2	1.76	-11.9%
Maximum number of on-state SMs	185	210	+13.5%
Sum of on-state SMs in each phase	200	227	+13.5%
Number of maximum tolerable faults	20	35	+75%
utilization ratio of SMs	84.1%	95.5%	+13.6%

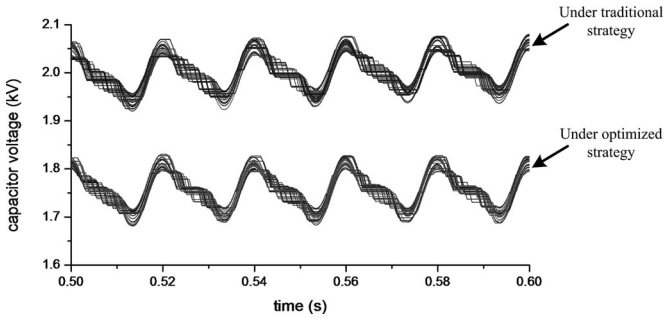

Fig. 8. Comparison of the capacitor voltage.

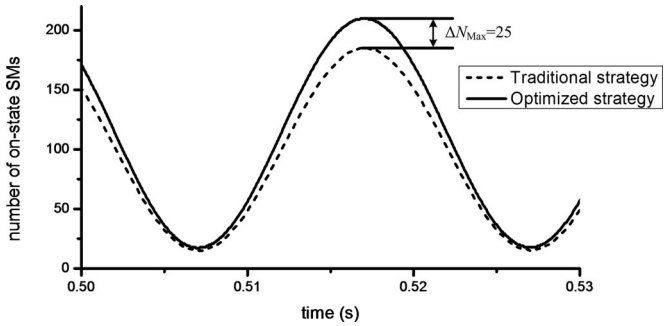

Fig. 9. Comparison of the number of on-state SMs.

B. Performance of the Steady-state Operation

According to the circuit parameters shown in Table I, $R_{\rm dc}$ is equal to 10% and $R_{\rm ac}$ is equal to 7.5%. Assuming the dynamic redundancy, $R_{\rm dynamic}$ is set to 5%; the comparison of some indexes under different strategies is shown in Table II. In particular, Figs. 8 and 9 show the comparison of the capacitor voltage and the number of the on-state SMs, respectively.

From the comparisons, it can be seen obviously that the capacitor voltage is reduced and the utilization ratio of the SMs is effectively improved.

C. Performance of the Dynamic Adjusting of Redundancy

In MMC-1, the voltage of the ac system is changed at $t = 1$ s. The modulation index m rises from 0.85 to 0.9 slowly, and the time for the process is 0.5 s. At $t = 2$ s, the dynamic redundancy is adjusted from 7% to 5%, the time for the process is 0.1 s. Fig. 10 shows the dynamic response of the system. The phase voltage at PCC-1 is depicted in Fig. 10(a) and 10(b)

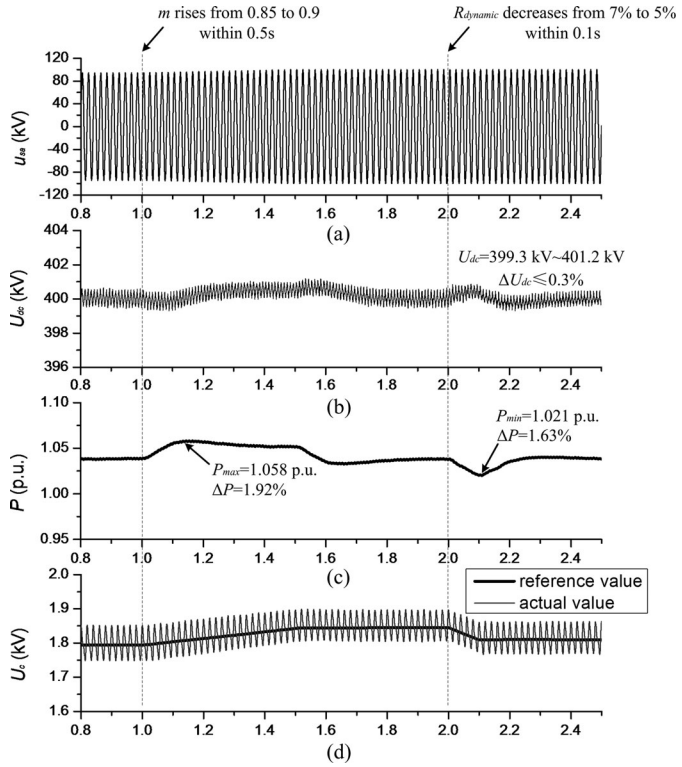

Fig. 10. Dynamic response of the system during the adjustment. (a) Phase voltage at PCC-1. (b) DC-bus voltage. (c) Active power at PCC-1. (d) Reference and actual average value of the capacitor voltage.

shows the dc-bus voltage. The active power at PCC-1 is shown in Fig. 10(c). The reference value and the actual average value of the capacitor voltage are shown in Fig. 10(d).

It can be seen that the reference value of the capacitor voltage is adjusted according to the different operating conditions, and it is followed accurately. During the adjustment, there is no obvious fluctuation on most of the system indexes. In fact, the change of the ac phase voltage usually takes a long time, and the dynamic redundancy needs not to be adjusted in a short time, so the system will have a better performance in actual operations.

D. Performance of the Fault Protection

In MMC-1, the modulation index m is set to 0.85 and the dynamic redundancy is set to 5%. Assuming that $N_{\rm dc}$ SMs have already malfunctioned in the upper arm of phase j, and there are only 200 available SMs in total. Unlike the traditional methods, the station needs not to be blocked. At $t = 1$ s, another four SMs fail. The bypass switches operate at $t = 1.005$ s and short out the faulted SMs. Then, the reference value of the capacitor voltage is adjusted in the next control cycle. Fig. 11 shows the transient behavior of the system during the fault. The phase voltage at PCC-1 is depicted in Fig. 11(a), Fig. 11(b) shows the current in the upper arm, Fig. 11(c) shows the dc-bus voltage, Fig. 11(d) shows the dc current in the positive pole, the active power at PCC-1 is shown in Fig 11(e), and Fig. 11(f) shows the reference value and the actual average value of the capacitor voltage.

As can be seen from Fig. 11, the dc-bus voltage drops after the fault occurred because of the instantaneous decrease in the

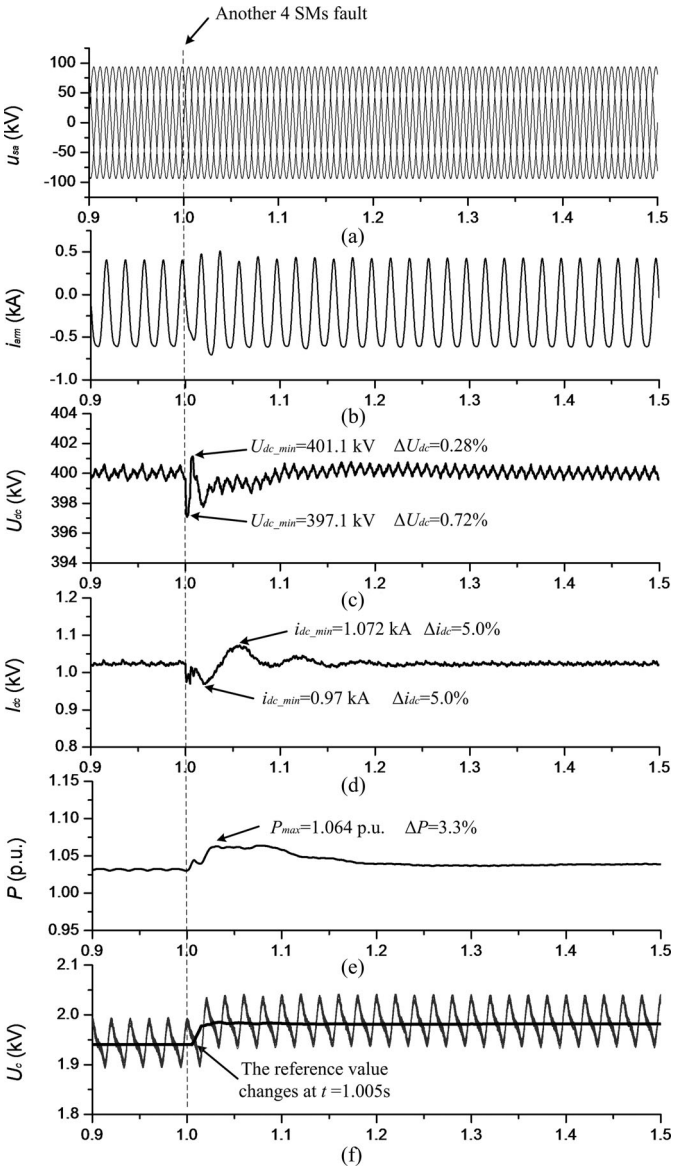

Fig. 11. Dynamic response of the system during the fault. (a) Phase voltage at PCC-1. (b) Current in the arm. (c) DC-bus voltage. (d) DC current in positive pole. (e) Active power at PCC-1. (f) Reference and actual average value of the capacitor voltage.

arm voltage, while the current in the dc bus and the converter arm fluctuates slightly. Under the influence of SM failures, the reference value of the capacitor voltage rises. In order to supply the extra energy absorbed by the capacitor, the active power absorbed from the ac system rises correspondingly. After the protection put in, the capacitor voltage automatically tracks the reference value and achieves the adjustment within 0.02 s. The system is nearly steady at around 1.1 s. As the most important index, the instantaneous drop of the dc-bus voltage is only 0.72%. The increasing rate of the active power is also acceptable, thus, the system has enough time to adjust. The fluctuation of $i_{\rm dc}$ is the biggest, but the maximum oscillation amplitude in the transient process does not exceed 5%, which can be tolerated by the system. Since malfunction of four SMs (2% of the arm SMs)

at the same time is seldom seen in real projects, the strategy proposed here can realize the protection in extreme cases.

VI. Conclusion

In this paper, the factors that influence the system operation, especially the number of the on-state SMs are analyzed. Considering the synthetical effects of the ac and dc systems, the dynamic redundancy and the utilization ratio of SMs are proposed as two novel indexes. On this basis, the optimized control strategy based on the dynamic redundancy for the MMC is discussed here.

As one of the main innovations, the calculation of the reference capacitor voltage is discussed in detail, and the modulation and protection method are improved correspondingly. A model of the MMC-HVDC system is built in PSCAD/EMTDC, and the simulation result proves the validity and feasibility of the proposed strategy. In this method, the capacitor voltage is reduced and the utilization ratio of SMs can be improved effectively. In addition, the safety margin can be adjusted dynamically, and the fault ride-through capability of the system can be enhanced.

References

[1] R. Marquardt, "Stromrichterschaltungen mit verteilten Energiespeichern," German Patent DE 10 103 031A1, Jan. 24, 2001.

[2] M. Glinka and R. Marquardt, "A new AC/AC multilevel converter family," *IEEE Trans. Ind. Electron.*, vol. 52, no. 3, pp. 662–669, Jun. 2005.

[3] S. Allebrod, R. Hamerski, and R. Marquardt, "New transformerless, scalable modular multilevel converters for HVDC-transmission," in *Proc. IEEE Power Electron. Spec. Conf.*, Jun. 15–19, 2008, pp. 174–179.

[4] M. Hagiwara and H. Akagi, "Control and experiment of pulsewidth-modulated modular multilevel converters," *IEEE Trans. Power Electron.*, vol. 24, no. 7, pp. 1737–1746, Jul. 2009.

[5] S. Rohner, S. Bernet, M. Hiller, and R. Sommer, "Modulation, losses, and semiconductor requirements of modular multilevel converters," *IEEE Trans. Ind. Electron.*, vol. 57, no. 8, pp. 2633–2642, Aug. 2010.

[6] M. Saeedifard and R. Iravani, "Dynamic performance of a modular multilevel back-to-back HVDC system," *IEEE Trans. Power Del.*, vol. 25, no. 4, pp. 2903–2912, Oct. 2010.

[7] M. Hagiwara, R. Maeda, and H. Akagi, "Control and analysis of the modular multilevel cascade converter based on double-star chopper-cells (MMCC-DSCC)," *IEEE Trans. Power Electron.*, vol. 26, no. 6, pp. 1649–1658, Jun. 2011.

[8] S. Shao, P. W. Wheeler, J. C. Clare, and A. J. Watson, "Fault detection for modular multilevel converters based on sliding mode observer," *IEEE Trans. Power Electron.*, vol. 28, no. 11, pp. 4867–4872, Nov. 2013.

[9] H. Huang, "Multilevel voltage-sourced converters for HVDC and FACTS applications," presented at the CIGRÉ SC B4 Bergen Colloq., Bergen, Norway, 2009.

[10] J. Dorn, H. Huang, and D. Retzmann, "A new multilevel voltage-sourced converter topology for HVDC applications," in *Proc. Conf. Int. Des Grands Reseaux Electriques*, 2008, pp. 1–8.

[11] G. S. Konstantinou, M. Ciobotaru, and V. G. Agelidis, "Effect of redundant sub-module utilization on modular multilevel converters," in *Proc. IEEE Int. Conf. Ind. Technol.*, Mar. 19–21, 2012, pp. 815–820.

[12] T. Qingrui and X. Zheng, "Impact of sampling frequency on harmonic distortion for modular multilevel converter," *IEEE Trans. Power Delivery*, vol. 26, no. 1, pp. 298–306, Jan. 2011.

[13] Z. Li, P. Wang, H. Zhu, Z. Chu, and Y. Li, "An improved pulse width modulation method for chopper-cell-based modular multilevel converters," *IEEE Trans. Power Electron.*, vol. 27, no. 8, pp. 3472–3481, Aug. 2012.

[14] K. Ilves, A. Antonopoulos, S. Norrga, and H. P. Nee, "A new modulation method for the modular multilevel converter allowing fundamental switching frequency," *IEEE Trans. Power Electron.*, vol. 27, no. 8, pp. 3482–3494, Aug. 2012.

[15] L. Harnefors, A. Antonopoulos, S. Norrga, L. Angquist, and H. P. Nee, "Dynamic analysis of modular multilevel converters," *IEEE Trans. Ind. Electron.*, vol. 60, no. 7, pp. 2526–2537, Jul. 2013.

[16] K. Ilves, A. Antonopoulos, S. Norrga, and H. P. Nee, "Steady-state analysis of interaction between harmonic components of arm and line quantities of modular multilevel converters," *IEEE Trans. Power Electron.*, vol. 27, no. 1, pp. 57–68, Jan. 2012.

[17] M. Guan and Z. Xu, "Modeling and control of a modular multilevel converter-based HVDC system under unbalanced grid conditions," *IEEE Trans. Power Electron.*, vol. 27, no. 12, pp. 4858–4867, Dec. 2012.

[18] D. Fujin and C. Zhe, "A control method for voltage balancing in modular multilevel converters," *IEEE Trans. Power Electron.*, vol. 29, no. 1, pp. 66–76, Jan. 2014.

[19] C. Gao, X. Jiang, Y. Li, Z. Chen, and J. Liu, "A DC-Link voltage self-balance method for a diode-clamped modular multilevel converter with minimum number of voltage sensors," *IEEE Trans. Power Electron.*, vol. 28, no. 5, pp. 2125–2139, May 2013.

[20] T. Qingrui, X. Zheng, C. Yong, and G. Li, "Suppressing DC voltage ripples of MMC-HVDC under unbalanced grid conditions," *IEEE Trans. Power Del.*, vol. 27, no. 3, pp. 1332–1338, Jul. 2012.

[21] G. T. Son, H.-J. Lee, T. S. Nam, Y.-H. Chung, U.-H. Lee, S.-T. Baek, K. Hur, and J.-W. Park, "Design and control of a modular multilevel HVDC converter with redundant power modules for noninterruptible energy transfer," *IEEE Trans. Power Del.*, vol. 27, no. 3, pp. 1611–1619, Jul. 2012.

[22] T. Qingrui, X. Zheng, and X. Lie, "Reduced switching-frequency modulation and circulating current suppression for modular multilevel converters," *IEEE Trans. Power Del.*, vol. 26, no. 3, pp. 2009–2017, Jul. 2011.

[23] Q. Song, W. Liu, X. Li, H. Rao, S. Xu, and Licheng Li, "A steady-state analysis method for a modular multilevel converter," *IEEE Trans. Power Electron.*, vol. 28, no. 8, pp. 3702–3713, Aug. 2013.

[24] S. Kouro, R. Bernal, H. Miranda, C. A. Silva, and J. Rodriguez, "High-performance torque and flux control for multilevel inverter fed induction motors," *IEEE Trans. Power Electron.*, vol. 22, no. 6, pp. 2116–2123, Nov. 2007.

[25] K. Ilves, A. Antonopoulos, L. Harnefors, S. Norrga, L. Angquist, and H. P. Nee, "Capacitor voltage ripple shaping in modular multilevel converters allowing for operating region extension," in *Proc. IEEE 37th Annu. Conf. Ind. Electron. Soc.*, Nov. 7–10, 2011, pp. 4403–4408.

[26] Z. Li, P. Wang, Z. Chu, H. Zhu, Y. Luo, and Y. Li, "An inner current suppressing method for modular multilevel converters," *IEEE Trans. Power Electron.*, vol. 28, no. 11, pp. 4873–4879, Nov. 2013.

[27] U. N. Gnanarathna, A. M. Gole, and R. P. Jayasinghe, "Efficient modeling of modular multilevel HVDC converters (MMC) on electromagnetic transient simulation programs," *IEEE Trans. Power Del.*, vol. 26, no. 1, pp. 316–324, Jan. 2011.

Gaoren Liu was born in Tianjin, China, in May 1990. He received the B.S. degree in electrical engineering from Zhejiang University, Hangzhou, China, in 2012, where he is currently working toward the Ph.D. degree in electrical engineering.

His research interests include high-voltage direct current and flexible alternating current transmission systems applications.

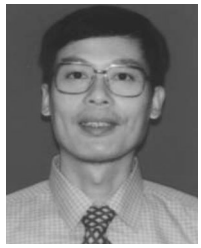

Zheng Xu (M'00) was born in Zhejiang, China, in September 1962. He received the B.S., M.S., and Ph.D. degrees in electrical engineering from Zhejiang University, Hangzhou, China, in 1983, 1986, and 1993, respectively.

He has been with the Department of Electrical Engineering, Zhejiang University, since 1986, and has been a Professor there since 1998. His research area includes high-voltage direct current, flexible alternating current transmission systems, and grid integration of renewable energy.

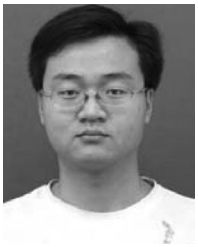

Yinglin Xue (S'13) was born in Hebei, China, in April 1986. He received the B.S. degree in electrical engineering from Zhejiang University, Hangzhou, China, in 2009, where he is currently working toward the Ph.D. degree in electrical engineering.

His main field of interest includes high-voltage direct current and flexible alternating current transmission systems.

Geng Tang was born in Fujian, China, in August 1988. He received the B.S. degree in electrical engineering from Zhejiang University, Hangzhou, China, in 2011, where he is currently working toward the Ph.D. degree in electrical engineering.

His main field of interest includes high-voltage direct current and flexible alternating current transmission systems.